# Exploring Mechanisms in Responders to Medication in Pulmonary Hypertension

Malak Sabry[1,2], Ahmed Hassan[2,3], Florinda Dilger[1], Chiemeka Nwandu[1], Magdi H Yacoub[2,5], Pablo Lamata[1], Adelaide de Vecchi[1]

[1] Department of Biomedical Engineering, King's College London, London, UK
[2] Aswan Heart Centre, Magdi Yacoub Foundation (MYF), Aswan, Egypt
[3] Cardiology Department, Cairo University, Cairo, Egypt
[4] National Heart and Lung Institute, Imperial College London, London, UK

## Abstract

*Treprostinil is a vasodilator approved for the treatment of Pulmonary Hypertension (PH). It dilates downstream blood vessels, reducing mean pulmonary arterial pressure (mPAP), peripheral vascular resistance (PVR), and right ventricular (RV) workload. This study combines clinical data and in-silico modelling to explore preliminary insights into commonalities among treatment responders. Pilot data from 4 PH patients who responded to therapy were analyzed, focusing on structural remodelling and pulmonary artery (PA) flow patterns. Previous literature suggested that the duration of a pathological vortex in the main PA trunk, $t_{vortex}$, correlates with mPAP, and the current study aims to test the hypotheses that $t_{vortex}$ is altered due to the dual action of change in PVR along with the corresponding remodelling, and that the closer the point is to the correlation line, the more adapted the system is. Findings indicate that, in the studied cases, while RV function and proximal PA geometry remained relatively unchanged after treatment, there was remodelling in distal vessels. mPAP and $t_{vortex}$ decreased after 6 months on medication. Consequently, the responders' haemodynamic state, as defined by mPAP and $t_{vortex}$, became aligned with the literature correlation line. The change in distance from the correlation line at follow-up was found to be inversely proportional to the starting distance, suggesting a potential diagnostic marker ($R^2 = 96\%$) to identify responders.*

## 1. Introduction

Pulmonary Hypertension (PH) is a chronic condition marked by an elevated mean pulmonary arterial pressure (mPAP) exceeding 20 mmHg at rest, leading to progressive vascular remodelling in the pulmonary arteries (PA) and eventual right ventricular (RV) dysfunction [1]. Both RV contractility and PA function must adapt to maintain an efficient system. Treprostinil, an approved vasodilator drug for Group I PH, reduces pulmonary vascular resistance and RV afterload by dilating downstream blood vessels, theoretically improving cardiac output within months [2]. While the drug normalizes RV function and afterload in some patients [3], it is ineffective in others, highlighting the need to predict irreversible RV failure and improve patient selection for Treprostinil accordingly.

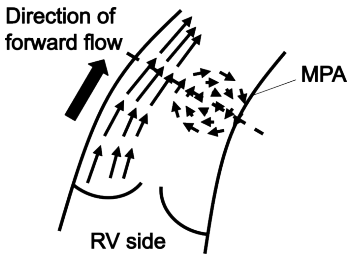


Figure 1. Vortex as described in the literature.

Recent studies have demonstrated an empirical link between mPAP and the duration of pathological vortex in the main PA (MPA) in PH patients. The vortex was identified through 4D Flow MRI as a concentric ring with tangential velocity vectors indicating simultaneous forward and backward flow [4, 5], as shown in Fig. 1. In previous work, an *in-silico* parametric study was conducted, exploring how inlet flow, afterload, and PA shape affected this correlation, and led to the hypothesis that the duration of the vortex seems to be driven by the interplay between the PA shape and the inflow from the RV, in turn depending on its contractility pattern. This suggests that points near the correlation line are cases where remodelling, either arterial or ventricular, has occurred along with the pressure changes. This study investigates the effect of Treprostinil on the remodelling and flow patterns using *in-silico* cardiovascular models, with the goal of understand the mechanisms linking changes in vortex duration and ventricular

mechanics in patients responding to medication.

## 2. Methods

### 2.1. Cohort

Data from 4 confirmed Group I PH patients responding to Treprostinil treatment were used for this study, including anatomical and flow imaging at their first visit, before drug administration, and after 6 months of treatment. In both visits, computed tomography (CT) and magnetic resonance imaging (MRI) were performed on the RV and PA. 4D Flow MR images of the PA were acquired using a 4D Flow package on a Siemens MAGNETOM Sola Fit. Cases 1 and 2 had 4D Flow MRI only at the initial visit, while cases 3 and 4 had data at both visits. Missing flow data was obtained using personalized Computational Fluid Dynamics simulations (CFD). Pressure traces were obtained using a Judkins right-heart catheter. All subjects participated under informed consent. Data access was granted through the Aswan Heart Centre Research Ethics Committee (REC code: 20210804MYFAHC-VAPH-20211025).

Table 1. Cohort details, at first visit and at their 6 months follow-up (mPAP in mmHg, PVR in WU, CO in L/min).

| Case | Visit | mPAP | PVR | CO | Score |
|---|---|---|---|---|---|
| 1 | 1 | 61 | 26 | 2.3 | |
| | 2 | 53 | 20 | 1.7 | 2 |
| 2 | 1 | 60 | 20 | 1.7 | |
| | 2 | 52 | 13 | 3.3 | 3 |
| 3 | 1 | 80 | 33 | 2.2 | |
| | 2 | 65 | 21 | 2.5 | 3 |
| 4 | 1 | 89 | 42 | 2.0 | |
| | 2 | 76 | 21 | 3.0 | 3 |

A combination of three criteria was used to determine if a patient was a responder from a haemodynamic point-of-view. A score out of 3 was calculated, where a 1 was added any time one of the following conditions was met:
1. Decrease in mean pulmonary arterial pressure (mPAP)
2. Decrease in pulmonary vascular resistance (PVR)
3. Increase in cardiac output (CO)

A patient with a score of 0 or 1, was deemed not responding, while cases with scores of 2 or 3 were considered responders. The cases, along with their response scores at follow-up are shown in Table 3.

### 2.2. Conceptual Framework

In a pilot study, the effect of RV ejection, afterload, and PA shape on the correlation between vortex duration, $t_{vortex}$, and mPAP, was investigated using *in-silico* modelling, in an attempt to gain a mechanistic understanding. Preliminary simulations results revealed that remodelling processes, either arterial or ventricular, and not acute changes in afterload, were the main drivers of $t_{vortex}$, as was expected. In the current work, we present the distance $d$ of each point P with an (mPAP, $t_{vortex}$) combination, to the correlation line as a metric of system adaptation, proposing that, the smaller the distance, i.e. the closer we are to the correlation line, the more remodelled the system is. A visual representation of this distance metric and its change at follow-up, $\Delta d$, is shown in Fig. 2. We quantified metrics for RV and PA remodelling, along with $t_{vortex}$ and distance changes, to test this hypothesis.

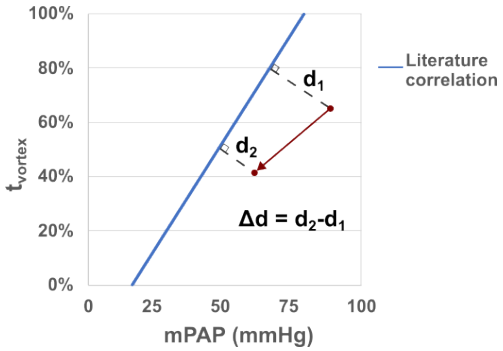


Figure 2. Visual representation distance at initial visit, $d_1$, follow-up distance, $d_2$, and their difference, $\Delta d$.

### 2.3. Morphological Remodelling

To evaluate RV remodelling at follow-up, functional parameters such as end-systolic and end-diastolic volumes (ESV and EDV), stroke volume (SV), and ejection fraction (EF) were quantified from MRI. To assess medication-induced vessel remodelling, 3D surfaces of the proximal PA, including the main trunk (MPA) and left and right branches (LPA, RPA), were manually segmented from CT images using 3D Slicer [6]. The Vascular Modelling Toolkit [7] was used to extract centerlines, and quantify the following geometric parameters of the PA anatomies in the 4 patients at initial and follow-up visits [8]: bifurcation angle, lengths and diameters of the PA segments.

### 2.4. Vortex Duration and Distance

Vortex duration time was inferred either by 4D Flow MRI, or by patient-specific CFD simulation, when imaging was unavailable. The 4D Flow Matlab toolbox [9] was used to process the data and visually identify the vortex from velocity vector fields, appearing as a concentric ring with tangential velocity vectors with simultaneous forward and backward flow in the same cross-section. $t_{vortex}$ was quantified as the percentage of frames where the vortex appears in the MPA over the total number of frames in the

imaging sequence. To quantify $t_{vortex}$ from CFD, a kinetic energy threshold in the vortex region was applied, as described in previous work, as it was not as straightforward to visually identify the vortex in CFD. The PA anatomy, with added outlet extensions for computational stability, was meshed using approximately 2 million tetrahedral elements, along with a prismatic boundary layer for near-wall resolution, following mesh independence. A velocity boundary condition was applied at the MPA inlet, extracted from 2D Flow MRI data at a plane above the pulmonary valve. At the LPA and RPA outlets, 3-element Windkessel models were applied and tuned to outflow rates from 2D Flow MRI at the respective branch levels. Blood was modelled as an incompressible Newtonian fluid ($\rho$ = 1060 Kg/m3, $\mu$ = 0.004 Pa.s). The Navier-Stokes equations were solved transiently in the fluid domain using ANSYS Fluent [10]. The distance d from the correlation line with equation $Ax+By+C=0$, for each point coordinates $(x_1, y_1)$ = (mPAP, $t_{vortex}$), was calculated as:

$$d = \frac{|Ax_1 + By_1 + C|}{\sqrt{A^2 + B^2}} \quad (1)$$

# 3. Results

## 3.1. Remodelling Metrics

RV function was quantified and shown in Table 2. In cases 2-4, EF increased slightly ($\leq$ 5%), while in case 1 the increase was of 12%. The RV volumes at ED and ES changed by less than 15% after 6 months on medication.

Table 2. RV functional parameters at first visit and at follow-up. Volumes are in mL.

| Case | Visit | EDV | ESV | EF |
|---|---|---|---|---|
| 1 | 1 | 455 | 388 | 0.15 |
| | 2 | 457 | 381 | 0.17 |
| 2 | 1 | 290 | 151 | 0.47 |
| | 2 | 331 | 172 | 0.48 |
| 3 | 1 | 360 | 257 | 0.29 |
| | 2 | 378 | 265 | 0.30 |
| 4 | 1 | 224 | 139 | 0.38 |
| | 2 | 206 | 128 | 0.38 |

Table 3 shows the changes in bifurcation angle, MPA mean diameter, and the ratio of change in RPA and LPA diameters over change in MPA diameter. In all four cases the change in LPA diameter was 2.7 to 4.2 times more important than the change in MPA diameter, as shown in the $\Delta D_L/\Delta D_M$ ratio. The changes in MPA diameter are all below 5%, while bifurcation angle changes range from around 2% to around 30%. These changes in shape features, along with the ratios seem to suggest that remodelling is mainly occurring in the downstream vasculature, and not as much in the MPA.

Table 3. Absolute percentage changes in bifurcation angle, $\alpha$, mean diameters, D, of the Main, Right and Left PAs (M, R, L), with change in RPA and LPA diameters over change in MPA diameter, $\Delta D_R/\Delta D_M$ and $\Delta D_L/\Delta D_M$.

| Case | $\Delta\alpha(\%)$ | $\Delta D_M(\%)$ | $\frac{\Delta D_R}{\Delta D_M}$ | $\frac{\Delta D_L}{\Delta D_M}$ |
|---|---|---|---|---|
| 1 | 22.5 | 1.7 | 3.3 | 3.3 |
| 2 | 30.7 | 0.8 | 0.2 | 4.1 |
| 3 | 2.2 | 2.8 | 2.4 | 4.2 |
| 4 | 8.0 | 4.4 | 0.3 | 2.7 |

## 3.2. Vortex Duration and Distance

Values of $t_{vortex}$, the distance from the line, d, and percentage changes are shown in Table 4. Fig. 3 shows each patient's trajectory in the (mPAP, $t_{vortex}$) plane.

Table 4. Vortex duration, $t_{vort.}$, distance from the correlation line, d, and percentage changes, $\Delta$.

| Case/Vis. | $t_{vort.}$ | d | $\Delta$mPAP | $\Delta t_{vort.}$ | $\Delta$d |
|---|---|---|---|---|---|
| 1/1 | 61% | 0.34 | -13.1% | -30.0% | -5.6% |
| 1/2 | 50% | 0.32 | | | |
| 2/1 | 43% | 0.50 | -13.3% | -35.0% | -11.5% |
| 2/2 | 36% | 0.44 | | | |
| 3/1 | 57% | 0.68 | -18.8% | -36.4% | -19.2% |
| 3/2 | 46% | 0.55 | | | |
| 4/1 | 51% | 0.85 | -14.6% | -50.0% | -17.6% |
| 4/2 | 45% | 0.70 | | | |

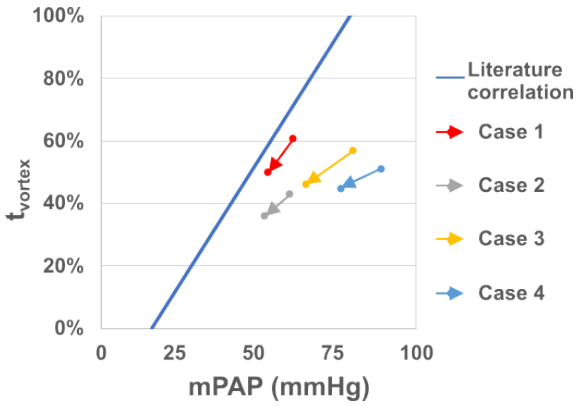


Figure 3. mPAP vs $t_{vortex}$ plot: correlation line shown in blue, trajectories of the studied cases shown as arrows.

All cases had a decrease in $t_{vortex}$, mPAP, and d at follow-up. The change in distance from the correlation line, $\Delta d$, was found to be highly correlated with the starting distance with an $R^2 = 0.96$. Initial distance was corre-

lated with changes in response biomarkers, namely mPAP ($R^2 = 0.65$) and PVR ($R^2 = 0.90$) (see Fig.4).

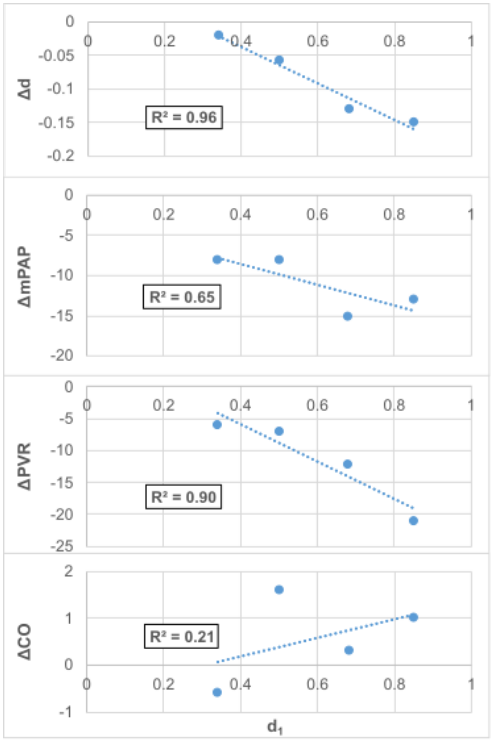


Figure 4. Initial distance vs change in response variables.

## 4. Discussion

In studied cases, Treprostinil appears to achieve its primary therapeutic objective—namely, the reduction of mPAP and PVR. Looking more closely at the mechanisms at play in these 4 responders, we see that with regards to RV function, cases had an improvement in EF of up to 12%, even in case 1 where RV was severely dilated and EF was very small (15%). Concerning PA shape, it was shown that across all subjects, changes in LPA diameter were notably more pronounced, ranging from 2 to 4 times greater than changes in the MPA diameter. This is consistent with Treprostinil's expected downstream remodelling effect, indicative of peripheral vascular adaptation. Concerning the $t_{vortex}$ analysis, at the initial visit, cases were to the right of the established mPAP–$t_{vortex}$ correlation line, implying that pressure increased but remodelling has not yet kept up. After 6 months, the data points converged closer to the correlation line, with reductions in both mPAP and $t_{vortex}$. Previous study results suggested that horizontal shifts on the plot correspond to acute changes in PVR without corresponding anatomical remodelling, whereas vertical shifts relate to PA structural remodelling and RV function changes. The observed trajectories support the dual action of Treprostinil: reducing afterload and initiating adaptive remodelling. Preliminary analysis of the change in distance from the correlation line revealed a strong linear relationship with the initial distance ($R^2 = 0.96$) in which the greater the initial distance, the more pronounced the response. This claim is reinforced by a strong correlation between initial distance and changes in response biomarkers, namely $\Delta$mPAP ($R^2 = 0.65$) and $\Delta$PVR ($R^2 = 0.90$). As this study was only conducted with 4 patients, all responders, with inconsistency in the imaging data availability, this correlation needs to be examined in further cases. If validated, it suggests a potential predictive marker: the therapeutic efficacy of Treprostinil may be greater in cases where remodelling has not yet occurred, i.e., early-stage intervention may yield more benefits.

## Acknowledgments

MS is funded by Siemens Healthineers and MYF.

## References

[1] Nakaya T, Ohira H, Sato T, Watanabe T, Nishimura M, Oyama-Manabe N, Kato M, Ito YM, Tsujino I. Rv–pa uncoupling and poor outcomes in PAH. Pulmonary Circulation 2020;10.

[2] Zare P, Heller D. Treprostinil. In StatPearls [Internet]. StatPearls Publishing, 2019; .

[3] Rischard F, Champion H, Vanderpool R, Waxman A, Hansen L, Jenkins I. Right vac in patients with pah undergoing rapid dose escalation of treprostinil. Journal of Heart Lung Transplantation 2014;33(4).

[4] Reiter G, Reiter U, Kovacs G, Kainz B, Schmidt K, Maier R, Olschewski H, Rienmueller R. Mr derived 3-d blood flow patterns in mpa as a marker of ph and a measure of elevated mpap. Circulation CVI 2008;.

[5] Reiter G, Reiter U, Kovacs G, Olschewski H, Fuchsjäger M. Blood flow vortices along the mpa measured with mr imaging for diagnosis of ph. Radiology 2014;275.

[6] 3d slicer. URL `https://www.slicer.org/`.

[7] Antiga L, Piccinelli M, Botti L, Ene-Iordache B, Remuzzi A, Steinman DA. An image-based modeling framework for patient-specific computational hemodynamics. Medical and Biological Eng and Computing 2008;46(11):1097–1112.

[8] Sabry M, Hermida U, Hassan A, Nagy M, Stojanovski D, Samuel I, Locas J, Yacoub MH, De Vecchi A, Lamata P. Exploring the relationship between pulmonary artery shape and pressure in ph. In STACOM. Springer Nature, 2024; .

[9] Sotelo J, Mura J, Hurtado D, Uribe S. A novel matlab toolbox for processing 4d flow mri data. International Society of Magnetic Reso nance in Medicine ISMRM 2019;.

[10] Ansys. URL `https://www.ansys.com/`.

Address for correspondence:
Malak Sabry, malaksabry@kcl.ac.uk
St Thomas' Hospital, London SE1 7EH, UK